

## Electronic Supplementary Information

### Details on deduction of guiding probabilities for simulation

The discrepancy between  $P_{\text{sim}}(\theta_a)$  and  $P_{\text{ex}}(\theta_a)$  resulted from the fact that, due to the difference in spatio-temporal resolution between the simulation and experiments, a single collision in experimental resolution can be resolved into multiple collisions in the simulation. Clemmens *et al.* set a criterion of a single collision in experiments: They did not count for multiple collisions unless microtubules traveled 0.5 $\mu\text{m}$  away from the boundary and then moved toward the same boundary for another collision<sup>1,2</sup>. Hence, guiding probability deduced from experiments should be considered as the summation of all contributions from all possible simulated paths within the region between the boundary and 0.5 $\mu\text{m}$  away from it.

To calculate each contribution, we considered a path as a combination of the following four components (Fig.S1):

- (1) Crossing the boundary with approach angle of  $\theta_a$ ;
- (2) Crossing the boundary again with crossing angle of  $\theta_w$  in the next time step after guided;
- (3) Leaving the boundary once, and crossing the boundary again with a crossing angle of  $\theta_b$  before reaching 0.5 $\mu\text{m}$  away from the boundary;
- (4) Leaving the boundary and reaching 0.5 $\mu\text{m}$  away from the boundary.

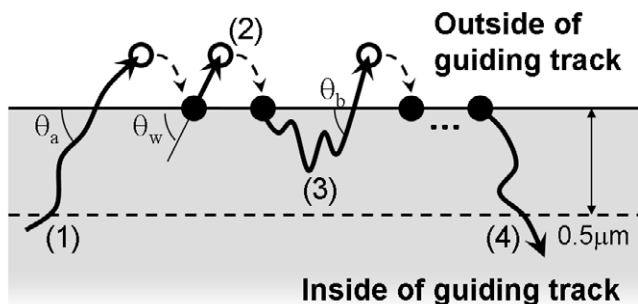


Figure S1. Schematic drawing of a path of a simulated microtubule with the region 0.5 $\mu\text{m}$  away from a track boundary

A trajectory with a single collision in experimental spatio-temporal resolution is one of possible combinations of the four components. Hence, the guiding probability deduced from experiments is the summation of all the possible combination.

The summation was performed as follows. For instance, Fig. S2 schematically shows two possible trajectories of a simulated microtubule crossing the boundary twice and reaching 0.5 $\mu\text{m}$  away from the boundary.

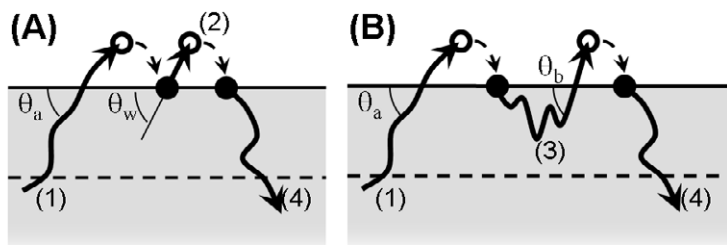


Figure S2. Schematic drawings of MT trajectories which cross the track boundary twice.

In the case of Fig. S2 (A), given  $\theta_w$ , the contribution from the path was given by the following:

$$P_{sim}(\theta_a) \cdot \frac{1}{2} \cdot P_{sim}(\theta_w) \cdot \frac{1}{2} \cdot (1 - p_b), \quad (1)$$

where  $p_b$  is the probability that a MT leaves a boundary once and then moved toward the same boundary for another collision without reaching  $0.5\mu\text{m}$  away from the boundary.  $p_b$  was obtained by running simulations to be 0.68. By averaging over all the possible  $\theta_w$ , the contribution was given by the following:

$$P_{sim}(\theta_a) \cdot \frac{1}{2} \cdot \langle P_{sim}(\theta_w) \rangle_{\theta_w} \cdot \frac{1}{2} \cdot (1 - p_b), \quad (2)$$

where  $\langle \dots \rangle_{\theta_w}$  stands for the average over the distribution of  $\theta_w$ . The distribution of  $\theta_w$  is a half-normal distribution.

In a similar manner, the contribution from the case of Fig. S2 (B) was given by the following:

$$P_{sim}(\theta_a) \cdot \frac{1}{2} \cdot p_b \cdot \langle P_{sim}(\theta_b) \rangle_{\theta_b} \cdot \frac{1}{2} \cdot (1 - p_b), \quad (3)$$

where  $\langle \dots \rangle_{\theta_b}$  stands for the average over the distribution of  $\theta_b$ . The simulation revealed that the distribution of  $\theta_b$  was well fitted with the log-normal distribution with the following formula:

$$f(\theta_b) = \frac{1}{\sqrt{2\pi} \cdot 0.89 \cdot \theta_b} \exp\left(-\frac{\left(\log\left(\frac{\theta_b}{2.85}\right)\right)^2}{2 \cdot (0.89)^2}\right). \quad (4)$$

After all, the contribution from paths crossing the boundary twice is obtained by adding equations (2) and (3):

$$P_{sim,2}(\theta_a) = P_{sim}(\theta_a) \cdot \left( \frac{1}{2} \cdot \langle P_{sim}(\theta_w) \rangle_{\theta_w} + \frac{1}{2} \cdot p_b \cdot \langle P_{sim}(\theta_b) \rangle_{\theta_b} \right) \cdot \frac{1}{2} \cdot (1 - p_b). \quad (5)$$

In the similar manner, one can calculate the contribution from paths crossing the boundary  $i$  times as:

$$P_{sim,i}(\theta_a) = P_{sim}(\theta_a) \cdot \left( \frac{1}{2} \cdot \langle P_{sim}(\theta_w) \rangle_{\theta_w} + \frac{1}{2} \cdot p_b \cdot \langle P_{sim}(\theta_b) \rangle_{\theta_b} \right)^{i-1} \cdot \frac{1}{2} \cdot (1 - p_b). \quad (6)$$

After all, since  $P_{ex}(\theta_a)$  is the summation of all the possible paths,

$$\begin{aligned} P_{ex}(\theta_a) &= \sum_{i=1}^{\infty} P_{sim,i}(\theta_a) \\ &= \sum_{i=1}^{\infty} P_{sim}(\theta_a) \cdot \left( \frac{1}{2} \cdot \langle P_{sim}(\theta_w) \rangle_{\theta_w} + \frac{1}{2} \cdot p_b \cdot \langle P_{sim}(\theta_b) \rangle_{\theta_b} \right)^{i-1} \cdot \frac{1}{2} \cdot (1 - p_b) \\ &= \frac{P_{sim}(\theta_a) \cdot (1 - p_b)}{2 - \langle P_{sim}(\theta_w) \rangle_{\theta_w} - p_b \cdot \langle P_{sim}(\theta_b) \rangle_{\theta_b}}. \end{aligned} \quad (7)$$

$P_{sim}(\theta_a)$  is not able to be deduced only with eq.(7), since it requires averages of unknown  $P_{sim}(\theta_a)$ . However, from the above expression, one can tell that  $P_{ex}(\theta_a) \propto P_{sim}(\theta_a)$ . Hence,

$$P_{sim}(\theta_a) = \alpha \cdot P_{ex}(\theta_a), \quad (8)$$

where  $\alpha$  is a constant. If  $P_{sim}(\theta_a) > 1$ ,  $P_{sim}(\theta_a)$  was set to be 1. We solved the equation (7) in a self-consistent manner with the equation (8). That is, substituting the equation (8) into the equation (7),  $\alpha$  was numerically determined.

### Supplemental information on reproduction of guiding probability with experimental spatio-temporal resolution

#### Reproduction of Guiding Probabilities of Gold Tracks with PEG blocked SiO<sub>2</sub> barriers

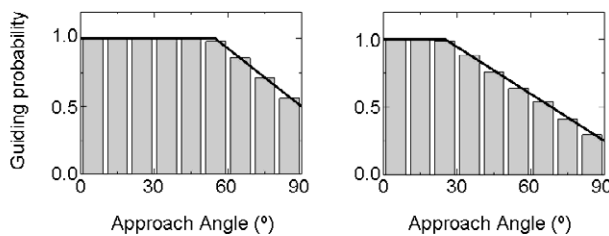


Figure S3. Reproduction of guiding probabilities of gold tracks with PEG blocked SiO<sub>2</sub> barriers<sup>3</sup>. (Left) Gold tracks with high kinesin density; (Right) Gold tracks with low kinesin density. Solid lines show guiding probabilities deduced from the experiment: (Left)  $y = 125/70 - x/70$ ; (Right)  $y = 335/260 - 3x/260$ .

#### Additional Validation of Calculated Values of $\alpha$

To further validate our method of deducing guiding probabilities for the simulation, the optimum values of  $\alpha$  was parametrically searched and compared with those obtained with the numerical deductions described above. Figure S4 shows square residues between histograms obtained from experiments<sup>1,3</sup> and those reproduced with the simulation with various  $\alpha$ . The values of  $\alpha$  which gave the least square residues showed good agreements with those calculated with the method reported in this paper.

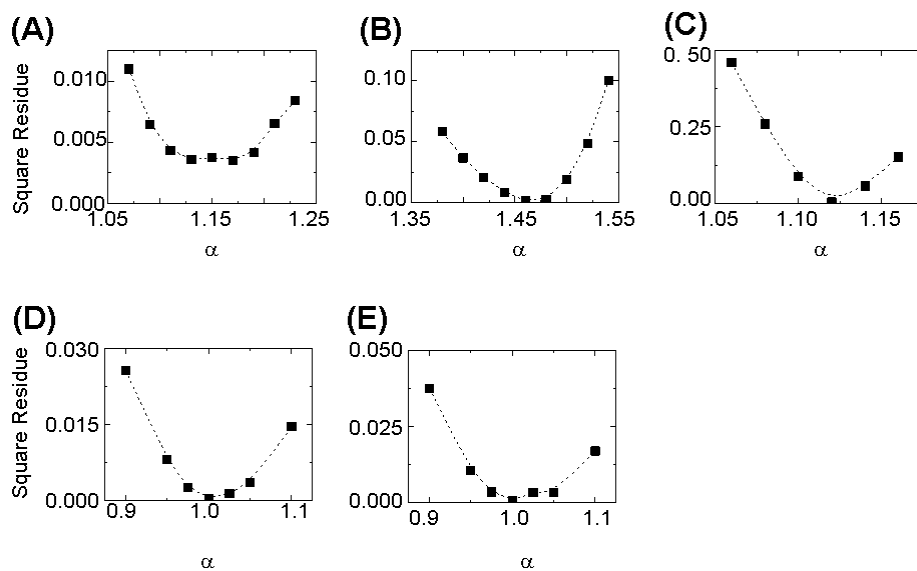


Figure S4. Square residues of reproduced histograms from experimental regression curves as a function of manually adjusted  $\alpha$ . (A) ppPEO chemically patterned track<sup>1</sup>; (B) PU topographical barrier<sup>1</sup>; (C) SiO<sub>2</sub> track with PEO-coated SU8-2 barriers<sup>1</sup>; (D) gold track with PEG-blocked SiO<sub>2</sub> barriers (high kinesin density)<sup>3</sup>; (E) gold track with PEG-blocked SiO<sub>2</sub> barriers (low kinesin density)<sup>3</sup>.

#### On the discrepancy in the distribution of $\theta$ in straight channel with the width of 5.5 $\mu$ m

The apparent discrepancy between the distribution of  $\theta$  obtained from the simulations and that from the experiment can be explained by the fact that the limited number of data set was analyzed in the experiment ( $N \approx 30$ ). Histograms of simulated collision angles were made from subset of whole collision data. The number of data in each subset was 30, which is comparable to that analyzed by Clemmens *et al.*<sup>2</sup> Figure S5 shows the comparison between the average histogram with standard deviation and the histogram reported by Clemmens *et al.*<sup>2</sup> The average and the standard deviation were calculated from 161 histograms constructed from the subset. Both histograms were fairly close

each other.

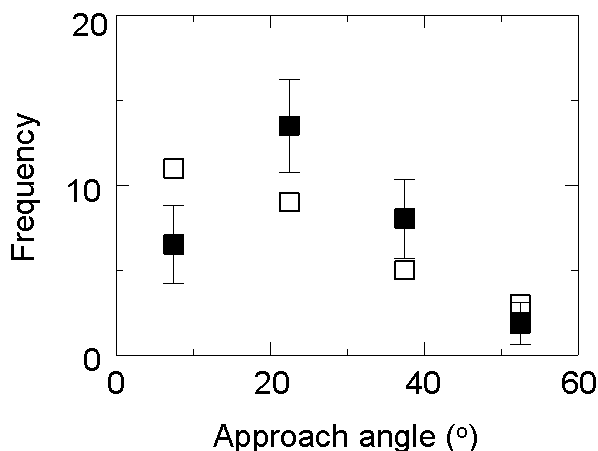


Figure S5. Histograms of approach angle of microtubules against topographical barriers in straight channels with the width of  $5.5\mu\text{m}$ . Solid squares, simulated microtubule movements (mean $\pm$ SD). Open squares, the experimental data of Clemmens *et al.*<sup>2</sup> was read and replotted.

## References

1. J. Clemmens, H. Hess, R. Lipscomb, Y. Hanein, K. F. Bohringer, C. M. Matzke, G. D. Bachand, B. C. Bunker and V. Vogel, *Langmuir*, 2003, **19**, 10967-10974.
2. J. Clemmens, H. Hess, J. Howard and V. Vogel, *Langmuir*, 2003, **19**, 1738-1744.
3. M. G. van den Heuvel, C. T. Butcher, R. M. Smeets, S. Diez and C. Dekker, *Nano Lett*, 2005, **5**, 1117-1122.